

Molecular Line Absorption in a Scattering Atmosphere. Part I: Theory

GRAEME L. STEPHENS AND ANDREW HEIDINGER*

Department of Atmospheric Science, Colorado State University, Fort Collins, Colorado

(Manuscript received 10 February 1998, in final form 1 July 1999)

ABSTRACT

This paper revisits the classical problem of particle scattering–gaseous absorption and considers the extent to which the growth of absorption lines of a known gas can be used to obtain information about the scattering particles. The focus of the study is directed toward interpretation of the reflection spectrum of the O₂ A band located in the spectral region between 0.759 and 0.771 μm and the results provide a theoretical foundation for the retrieval of particle information described in a related study. This study demonstrates that there are six main properties that affect the absorption and reflection spectra: the optical depth of the cloud or aerosol, the pressure level of the top of this layer, the (pressure) thickness of the layer, the scattering phase function, the particle single-scatter albedo, and the surface albedo. Measured quantities, such as the spectral radiance or the ratio of in-absorption to continuum radiances are shown to be sensitive to these parameters in a manner that varies according to the O₂ optical depth. This variation sensitivity offers a way of separating the dependence of the measurements on these parameters, thereby providing some basis for their retrieval with suitable spectral measurements that resolve a sufficient range of O₂ optical depth. Specifically, it is shown that radiances reflected from thin layers are sensitive to optical depth and phase function whereas the radiance ratio is sensitive to layer height. For thick layers, the sensitivity to optical depth diminishes leaving primarily a sensitivity to bulk information about the scattering phase function. By measuring radiances as a function of changing O₂ absorption, it is possible to distinguish optically thin layers above brighter lower reflecting surfaces, providing an ability to distinguish high-level thin cloud over brighter lower-level clouds or reflecting surfaces. The effects of 3D geometry on the spectral radiances is also considered in the context of photon path. It is shown how the spectral radiances provide some insight on 3D effects and the probable importance of these 3D effects on the retrievals. The equivalence theorem is illustrated and is used to provide line-by-line simulations of the reflection spectrum from hypothetical 3D clouds. A method to identify the nature of the 3D bias on retrievals of optical depth is discussed.

1. Introduction

The problem of radiative transfer in an atmosphere that exhibits both multiple scattering and gaseous absorption is relevant to a number of topics in both the atmospheric and climatic sciences. This problem is usually dealt with by dividing the spectral region of interest into a number of spectral bands that are narrow enough for the scattering properties to be taken as constant. Unfortunately, the gaseous absorption is most typically characterized by significant variability even over such narrow spectral regions. Methods such as the *k*-distribution approach and related techniques (e.g., Goody and Yung 1989; Lacis and Oinas 1991) are now widely used

to deal with gas absorption–particle scattering overlap over relatively broad spectral regions (regions typically broader than the bandpass of typical filter radiometers). Line-by-line simulations over a limited spectral range have been carried out to verify these procedures (Ramaswamy and Freidenreich 1991), but these studies are few in number and have not yet been extended over complete solar or terrestrial spectra.

The more classic problem underlying gas absorption–particle scattering overlap deals with the growth of line absorption under the influence of multiple scattering. Early interest in this problem stemmed from a desire to analyze planetary reflection spectra as a way of estimating the concentration of selected absorbing gases (see Chamberlain and Hunten 1987). A related problem has also been pursued in analyses of reflection spectra of the O₂ A band between 0.759 and 0.771 μm that might be obtained by an instrument viewing the earth. The remote sensing of the atmosphere based on sunlight reflected at wavelengths in the O₂ A band has a relatively long history (see O'Brien and Mitchell 1992) and most of this activity was motivated by the desire to estimate cloud-top pressure (Yamamoto and Wark 1961;

* Current affiliation: NOAA/NESDIS office of Research and Applications, Washington, D.C.

Corresponding author address: Dr. Graeme L. Stephens, Department of Atmospheric Science, Colorado State University Fort Collins, CO 80523.
E-mail: stephens@atmos.colostate.edu

Wu 1985; Fischer and Grassl 1991, among others) or surface pressure (e.g., Mitchell and O'Brien 1987).

This paper approaches the problem of interpretation of O_2 reflection spectrum in a manner different from these earlier studies. The intent of the study described in this paper is to revisit the classical problem of particle scattering–gaseous absorption and to consider the extent to which line absorption properties can be used to obtain information about the scatterers. One of the problems associated with retrieval of particle information from A-band spectra concerns how to separate the absorption by gases from the scattering by particles. O'Brien and Mitchell (1992) conclude that the O_2 spectrum itself, if observed with sufficient spectral resolution, contains information sufficient to deconvolve these effects and by implication provide a clearer view of the nature of the scattering. They argue that a spectral resolution of approximately 1 cm^{-1} is needed, which is significantly higher than currently exists for the Global Ozone Monitoring Experiment (e.g., Chance et al. 1997) and significantly higher than typically considered in past studies (e.g., Wu 1985; Fischer and Grassl 1991).

Although the topic of interest deals with interpreting the absorption spectrum of oxygen, the concepts introduced may also be applied to other gases, such as water vapor (Liou et al. 1997). The results presented below provide the theoretical foundation for the retrieval of particle information from spectral measurements of line absorption. A specific approach to retrieval using A-band radiances is presented in a related paper (Heidinger and Stephens 2000: hereafter Part II). The next section provides some background on the O_2 absorption spectrum and is followed by a simple atmospheric model of this absorption. This model is then incorporated into simple scattering models to identify the principal factors that influence solar reflection in the O_2 A band. This simple model serves to interpret the sensitivity results derived from a more complex model as presented in section 5. One of the key results of this analysis is that the sensitivities vary according to the strength of the O_2 absorption stated in terms of the column O_2 optical depth, and it is the variation of these sensitivities across the A-band spectrum that is the key to the retrieval methods introduced in Part II. Section 6 of the paper looks at the issue of the effects of three-dimensional transport on interpretation of these radiances and shows how the reflection spectrum itself contains meaningful information about these effects.

2. Background

The intent of the research described in this paper is to provide an understanding of the properties of absorbing lines formed in an oxygen atmosphere illuminated and viewed from above. The specific goal is to understand how these properties are influenced by particle scattering. The relation between the two (i.e., between line absorption and particle scattering) serves as

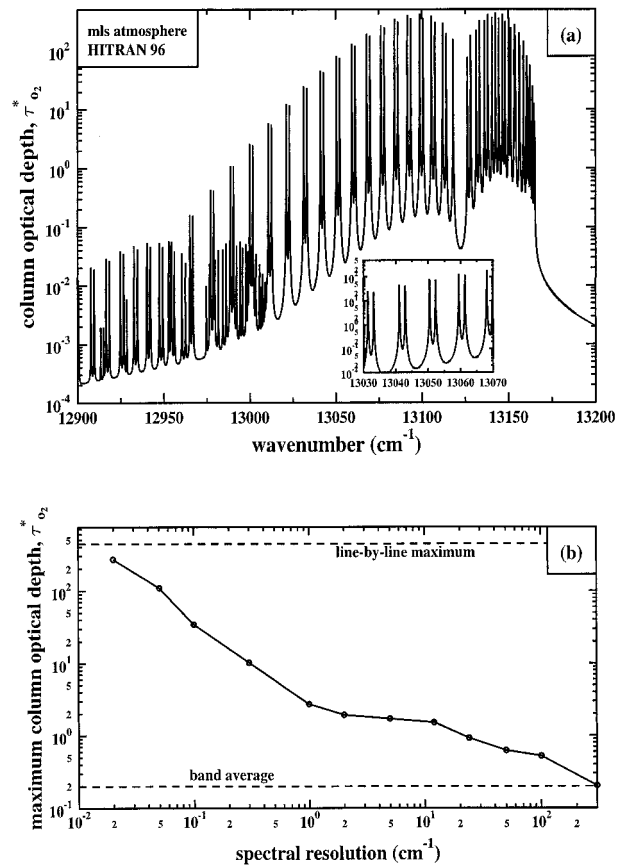


FIG. 1. Spectral variation of column optical depth in the O_2 A-band for standard midlatitude summer (m/s) atmosphere (a). Variation of maximum channel column optical depth as a function of instrument resolution (b).

a basis for the cloud and aerosol property retrievals of Part II.

One of the parameters that proves useful in discussing the connections between particle properties and the measured spectral radiances is the column optical depth of oxygen. This will be considered to be a known quantity governed by known spectral absorption properties and surface pressure (also assumed to be known). Figure 1a presents an example of the spectrum of this optical depth derived for the McClatchey et al (1972) midlatitude summer atmosphere and shown at a resolution of 0.001 cm^{-1} . The spectrum was derived using the Voigt line shape and line parameters taken from HITRAN 96 (see Rothman et al. 1987). The narrow absorption lines (of order 0.05 cm^{-1}) occurring in singlet and doublet pairs are highlighted in the inset and the characteristic P and R branches of the A-band spectrum are well illustrated.

Although it is not necessary to profile individual absorption lines for retrieval purposes it is necessary to resolve the absorption features beyond the capabilities of existing satellite instruments.

The range in column optical depth spans approximately seven orders of magnitude. In reality, however,

an instrument will possess a spectral response function that is broader than the width of an individual line effectively smoothing over these spectral lines and thereby reducing the range of optical depths that than can be resolved. This is highlighted in Fig. 1b, showing the maximum optical depth that is effectively sampled as a function of changing instrument resolution. For this purpose, the results shown were derived by fitting a single exponential form of transmission to the band-averaged transmission calculated from HITRAN at the stated resolution. A useful way of interpreting this diagram is as follows. A column O₂ optical depth of about 2 is the minimum required to remove contributions of surface reflection from the measured radiances. Thus a spectrometer with spectral resolution coarser than cm⁻¹ smears out the line profile and will not be able to resolve absorption in the stronger lines sufficiently to remove unwanted surface effects.

3. A simple model of O₂ line absorption

From an observational perspective, we study the line absorption properties in terms of measured spectral radiances and the related absorption profile

$$s_\nu = \frac{I_c - I_\nu}{I_c}, \quad (1)$$

where I_c is the radiance detected at the top-of-the-atmosphere at wavelengths out of the absorption line (i.e., in the continuum) and I_ν is the radiance measured in the line at frequency ν .

In this study we explore the relation between I_ν and s_ν and relevant particle scattering parameters as a function of changing O₂ optical depth. We introduce these relations in reference to a three-layer atmosphere as shown in Fig. 2. This atmosphere overlies a reflecting surface of albedo α_{sfc} . The vertical coordinate defining the location of the layers is the scaled pressure $\bar{p} = p/p_s$ where p is pressure and p_s is a suitable reference pressure. Each layer is defined by two pressures, \bar{p}_i and \bar{p}_{i+1} , specifying the upper and lower levels of the layer, respectively.

The absorption coefficient for an absorbing gas at pressure \bar{p} is

$$k_\nu(\bar{p}) = \frac{S(T)}{\alpha_s \pi} \frac{\bar{p}}{[f^2 + \bar{p}^2]} \quad (2)$$

where $f = \nu/\alpha_s$ and the half-width α_s is defined relative to a reference pressure p_s . The element of path is

$$du = \frac{r}{g} p_s d\bar{p}, \quad (3)$$

where r is the mixing ratio. With the assumption

$$rS = \text{constant}, \quad (4)$$

which approximately applies to uniformly mixed absorbing gases like O₂ and strictly to such a gas under

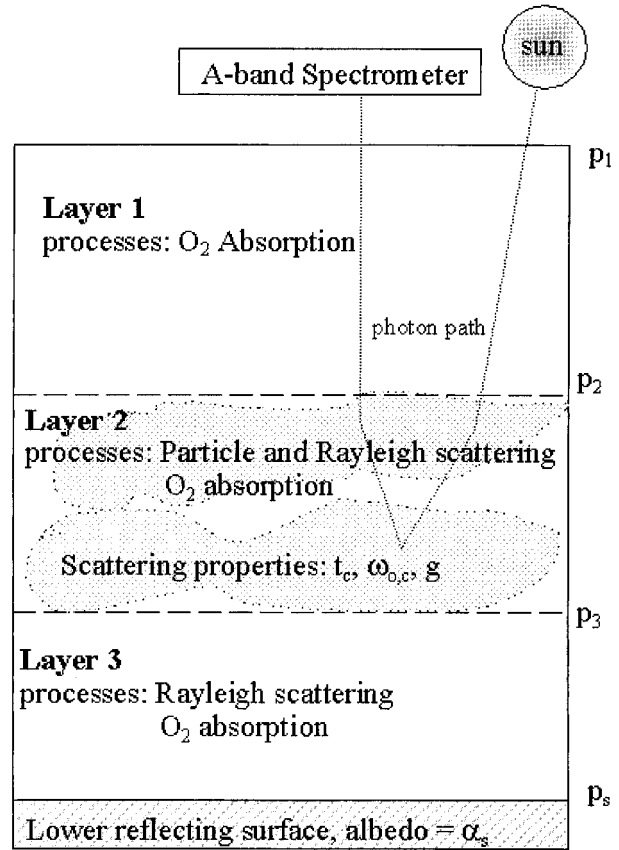


FIG. 2. Schematic diagram of hypothetical three-layer atmosphere showing relevant scattering and absorbing constituents in each layer.

isothermal conditions (S constant). Given this assumption, the optical depth of the layer $\bar{p}_i \rightarrow \bar{p}_{i+1}$ is

$$\tau_\nu(\bar{p}_i, \bar{p}_{i+1}) = k_s u_s \int_{\bar{p}_i}^{\bar{p}_{i+1}} \frac{\bar{p}}{f^2 + \bar{p}^2} d\bar{p} \quad (5)$$

where $k_s = S/\alpha_{\text{sfc}} \pi$ and where

$$u_s = r p_s / g \quad (6)$$

is the column path of absorbing gas. Evaluation of integral of (5) leads to

$$\tau_\nu(\bar{p}_i, \bar{p}_{i+1}) = \frac{k_s u_s}{2} \ln \left[\frac{\bar{p}_{i+1}^2 + f^2}{\bar{p}_i^2 + f^2} \right]. \quad (7)$$

The absorption profile for a purely gaseous atmosphere above a diffusely reflecting surface at pressure p_s thus follows from combination of (1) and (7)

$$s_\nu = 1 - \exp[-m\tau_\nu(0, 1)], \quad (10)$$

where

$$m = \left(\frac{1}{\mu_\odot} + \frac{1}{\mu} \right) \quad (11)$$

is the airmass factor with μ representing the cosine of

the zenith angle of observation and μ_\odot representing the cosine of the solar zenith angle.

The total optical depth of the atmosphere is

$$\tau_v^* = \tau_v(0, 1) + \tau_c,$$

where

$$\tau_v(0, 1) = \tau_v(0, \tilde{p}_1) + \tau_v(\tilde{p}_1, \tilde{p}_2) + \tau_v(\tilde{p}_2, 1)$$

is the total column optical depth of the absorbing gas and τ_c is the column optical depth of particles. It is convenient to introduce the optical depth of the atmosphere above the scattering layer in question as $t_v(0, \tilde{p}_i)$, where \tilde{p}_i is the pressure of the top of the scattering layer (in this case \tilde{p}_i corresponds either to \tilde{p}_1 or \tilde{p}_2). For the simulations shown later and in Part II that deal specifically with absorption in the O₂ A band, $\tau_{O_2}^*$ will be used in place of $\tau_v(0, 1)$ to represent the total column optical depth due to gaseous absorption.

4. Line profile formation in a mixed scattering–gaseous atmosphere

The line-absorption model above is now applied in two simple scattering models as a way of identifying the particle parameters that may possibly be retrieved from the measured radiances I_ν and the line profile s_ν . These models also provide a framework for understanding the series of sensitivities results described in the next section. Two simple scattering models are used for this purpose, the thin (i.e., $\tau_c \rightarrow 0$) and semi-infinite (i.e., $\tau_c \rightarrow \infty$) particle optical depth limits.

a. Thin (scattering) atmosphere approximation

Consider an optically thin Rayleigh scattering continuum of optical depth τ_{RAY} that may be assumed to occur in the lowermost layer of the model atmosphere (e.g., Fig. 2) and particle scattering continuum of optical depth τ_p either occurring in the middle layer or imbedded in the lower Rayleigh layer. These optical depths are assumed to be constant across the entire oxygen A band thus defining the continuum optical depth, τ_c , such that $\tau_c = \tau_p$ when the particles are located in the middle layer above the Rayleigh scattering and $\tau_c = \tau_p + \tau_{\text{RAY}}$ when the particles are imbedded in the lower Rayleigh layer.

For the problem at hand, it is convenient to separate the radiance observed at the satellite into a surface term, I_{surf} , and an atmospheric term, I_{atm} ,

$$I_{\text{sat}} = I_{\text{surf}} + I_{\text{atm}} \quad (12)$$

such that with the use of (8) and (9),

$$I_{\text{surf}} = \frac{\alpha_{\text{sfc}}}{\pi} F_\odot \mu_\odot e^{-m\tau_v^*}, \quad (13)$$

where F_\odot and μ_\odot define the intensity and direction of the solar beam, respectively. In the thin limit, only primary scattered radiation from the atmosphere back to

the satellite is considered. This primary scattered radiation can also be expressed as (e.g., Stephens 1994)

$$I_{\text{atm}}(\mu) = \frac{F_\odot}{4\pi} e^{-m\tau_v(0, \tilde{p}_i)} P_i(\mu_\odot, \mu) \times \int_{\tau_v(0, \tilde{p}_i)}^{\tau_v(0, \tilde{p}_{i+1})} \varpi_{o,v}(\tilde{p}) e^{-m\tau_v(\tilde{p}_i, \tilde{p})} \frac{d\pi(\tilde{p}_i, \tilde{p})}{\mu}, \quad (14)$$

where \tilde{p}_i refers to the pressure of the upper level of the scattering layer, \tilde{p}_{i+1} is the pressure of the lower level of the layer, $P_i(\mu_\odot, \mu)$ is the phase function characteristic of the scatterers in the layer (for simplicity taken to be independent of \tilde{p}), and $\varpi_{o,v}(\tilde{p})$ is the single-scattering albedo at \tilde{p} defined as

$$\varpi_{o,v} = \frac{\varpi_{o,c}}{1 + r_s \frac{\tilde{p}}{f^2 + \tilde{p}^2}}, \quad (15)$$

where the quantity

$$r_s = \frac{k_s}{\sigma_c + \kappa_c}$$

is the ratio of the gas absorption to particle (mass) extinction coefficients where the particle extinction coefficient is the sum of the continuum scattering and absorption coefficients, σ_c and κ_c , respectively and the quantity

$$\varpi_{o,c} = \frac{\kappa_c}{\kappa_c + \sigma_c}$$

is the single-scatter albedo due to particle absorption.

For illustration, consider a simple case for which $\varpi_{o,v}$ is constant through the scattering layer. Integration of (14) leads to

$$I_{\text{atm}}(\mu) = \frac{F_\odot}{4\pi\mu} e^{-m\tau_v(0, \tilde{p}_i)} \varpi_{o,v} P_i(\mu_\odot, \mu) e^{-m\tau_v(\tilde{p}_i, \tilde{p}_{i+1})} m\tau_c, \quad (16)$$

assuming that $m\tau_c \ll 1$. Therefore the radiance at the satellite follows as a combination of (13) and (16). This simple model identifies the following parameters potentially controlling the growth of absorption lines in a scattering atmosphere: 1) the optical depth of the continuum, τ_c ; 2) the upper level \tilde{p}_i of the scattering layer that defines the O₂ optical depth above the scattering layer; 3) the surface albedo α_{sfc} ; 4) the scattering phase function $P_i(\mu_\odot, \mu)$; 5) the pressure thickness of the scattering layer $\tilde{p}_{i+1} - \tilde{p}_i$ or more precisely the optical depth of oxygen in this layer; and 6) the continuum single-scatter albedo, $\varpi_{o,c}$. In this study, $\varpi_{o,c}$ is assumed unity that is typical of cloud particles and some aerosols in the O₂ A band and the sensitivity of the growth of absorption lines to changes in $\varpi_{o,c}$ will not be shown.

Crucial to any retrieval scheme that uses input measurables in the form of either I_ν and s_ν is the sensitivity of these measurables to changes in these five parameters.

We show in the results below how these sensitivities vary according to the O_2 optical depth and it is the variation of these sensitivities across the spectrum that is the key to the retrieval methods introduced in Part II. Furthermore, the radiances I_ν are sensitive to changes in these parameters in a manner that differs from that of the absorption profile s_ν . This can be appreciated by the following simple example. Consider the case of scattering by a thin layer over a dark surface. In this case

$$I_c = \frac{F_\odot}{4\pi\mu} \varpi_{o,\nu} P_i(\mu_\odot, \mu) e^{-m\tau_\nu(0,\bar{p}_i)} m\tau_c \quad (17)$$

$$s_\nu = 1 - e^{-m\tau_\nu(0,\bar{p}_i)} \quad (18)$$

after combining (16) and (17) in (1). According to (13) and (16) and with $\alpha_{sc} = 0$, the spectral intensity detected by an instrument on a satellite varies linearly with τ_c , phase function, and ϖ , and depends on cloud-top pressure \bar{p}_i . The line profile, on the other hand, reduces to a simple form defined solely in terms of the amount of absorbing gas above the scattering layer as specified by \bar{p}_i and entirely independent of particle properties. This picture changes with the introduction of surface reflection in a manner discussed below.

b. Thick (semi-infinite) atmosphere approximation

The semi-infinite atmosphere approximation under the assumption of isotropic scattering is able to account for anisotropic scattering via the similarity transformation

$$\varpi'_o = \frac{(1-g)\varpi_o}{1-g\varpi_o} \quad (19)$$

where ϖ'_o is the scaled single-scatter albedo for isotropic scattering and g is the asymmetry factor of the scattering phase function. It follows that (Chandrasekhar 1960)

$$I_\nu = \frac{1}{4} \varpi'_o F \frac{\mu_\odot}{\mu + \mu_\odot} H(\varpi'_o, \mu) H(\varpi'_o, \mu_\odot) \quad (20)$$

where $H(\varpi_o, \mu)$ is the Chandrasekhar H function. Assuming the particles are conservatively scattering, the line profile follows from (1) and (20) as

$$s_\nu = 1 - \varpi'_o \frac{H(\varpi'_o, \mu) H(\varpi'_o, \mu_\odot)}{H(1, \mu) H(1, \mu_\odot)} \quad (21)$$

where $H(1, \mu)$ is the H function for conservative scattering.

Figures 3a and 3b graphically portray (20) and (21) as a function of column oxygen optical depth $\tau_{O_2}^*$ for two stated values of g used to calculate ϖ'_o . Also shown are the relationships derived from a doubling/adding model with $\tau_c = 500$. These results show how information about the phase function is contained in reflected radiances, more so than in s_ν , and especially over ranges of moderate values of $\tau_{O_2}^*$. The phase function enters the H function solutions (20) and (21) through the scal-

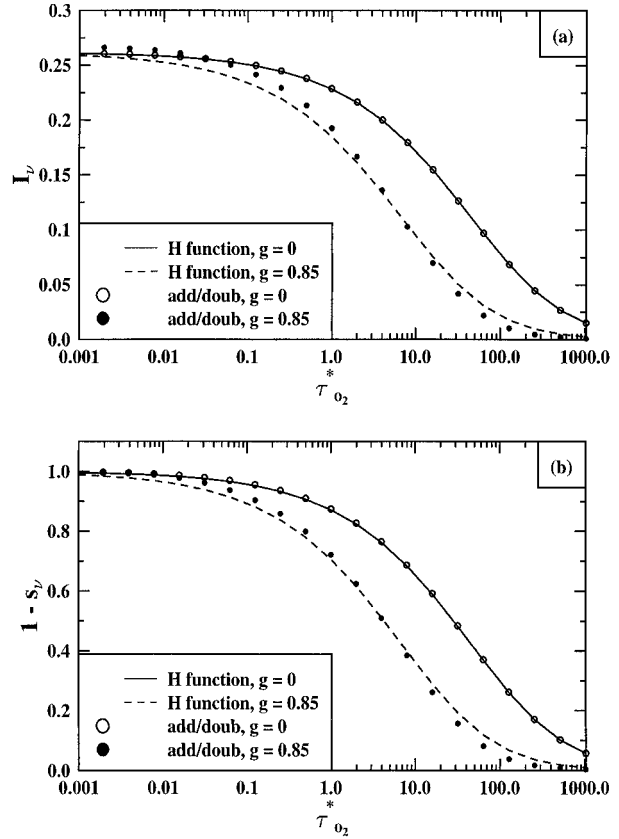


FIG. 3. Comparison of I_ν and s_ν between Chandrasekhar's H functions and an adding/doubling solution.

ing relationship (19) and then only in terms of g . This demonstrates that in the semi-infinite limit the reflected radiances depend only on bulk information about phase function (i.e., on g) and less so on detailed characteristics of the phase function as might be described by higher moments of a Legendre polynomial expansion. This is supported in the results of Figs. 4a and 4b, which reproduce the results of Fig. 3 with additional doubling/adding solutions derived using different forms of the double Henyey–Greenstein phase functions each with $g = 0.85$.

5. Sensitivity results

Sensitivity results are presented in terms of the following parameter

$$S_{ij} = \frac{\partial y_i}{\partial \ln x_j}, \quad (22)$$

which quantifies the amount that a given measurement y_i might be expected to change due to a given (percentage) change in the parameter x_j . In this case, y_i is either I_ν and s_ν and x_j is one of the five parameters identified above. The quantity S_{ij} , or closely related

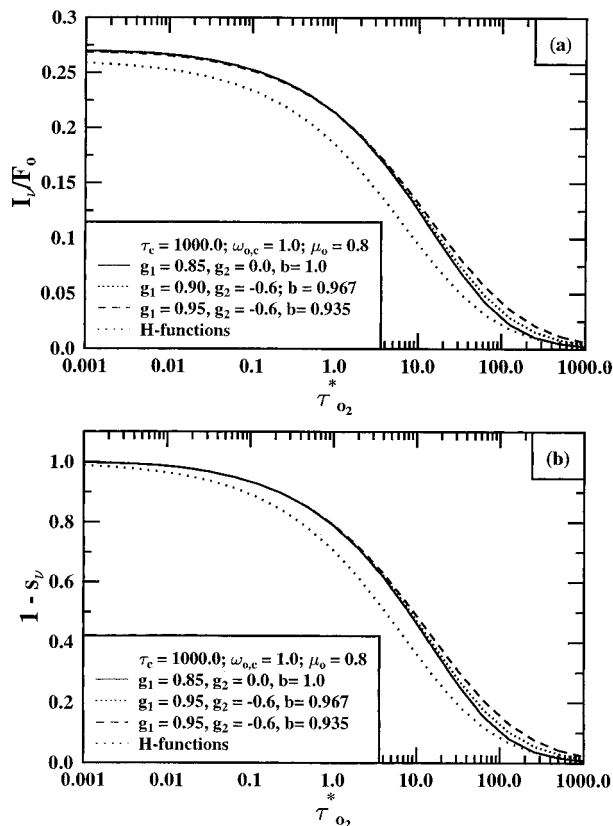


FIG. 4. Same as Fig. 3 except comparing results for differing double H-G phase functions with the same effective asymmetry parameter.

quantities, are integral to the retrieval method described in Part II.

Sensitivities were derived from simulations carried out with a doubling/adding model as a solution to the radiative transfer equation applied to the three-layer atmosphere of Fig. 2. For a scattering layer in the lower atmosphere, the simulations broadly represent a lower-tropospheric aerosol layer when optically thin and a low-level cloud when optically thick. The sensitivities derived for a scattering layer located in the upper atmosphere might be taken to apply to a cirrus cloud or perhaps a stratospheric aerosol layer. The optical properties assumed of the particles are that the particles are nonabsorbing across the A band and that the phase function is represented by a simple double Henyey–Greenstein function. The latter is characterized by the asymmetry parameter taken to be $g = 0.85$ unless otherwise stated. While the quantitative aspects of these sensitivities depend on the particular choices of optical properties, the qualitative differences and the way the sensitivities vary with the O_2 optical depth does not change significantly.

Figure 5 is an example of the sensitivities derived for an optically thin layer ($\tau_c = 0.1$) located with its upper pressure level at $\bar{p} = 0.35$ overlying a dark surface $a_{\text{sfc}} = 0$. The reflected radiances I_v and the line profile s_v ,

are presented as a function of the column oxygen optical depth $\tau_{O_2}^*$ as are the sensitivities S_{ij} . Presentation of results in this way merely represents a reorganization of the spectral information from lowest to highest values of O_2 optical depth. The interpretation of the sensitivities for the optically thin continuum follows according to the previous discussion of (17) and (18). The sensitivity of the reflected radiance is governed by changes in cloud-top pressure (the sensitivity is negative since an increase in the pressure leads to reduced radiances) and changes in optical depth and phase function. The latter influence the radiances in an approximate equal way as predicted by (16). It is important to note, however, that the optical depth–phase function sensitivity is largest in weak oxygen lines (or in regions of weak O_2 absorption) whereas the cloud-top pressure is increasingly more sensitive for the more opaque atmosphere with a maximum sensitivity occurring $\tau_{O_2}^* \approx 4$. In contrast, the line profile is sensitive only to changes in cloud-top pressure, which was also predicted by (18).

Although the sensitivities become more complex when surface reflection is included, the important point of these results remains that the sensitivities of the measurements to changes in the parameters vary according to the strength of the O_2 absorption. Thus, spectral measurements that resolve the range in absorption therefore offer potential for separating the dependence of the measurements on these parameters thereby providing some basis for their retrieval. These results are translated quantitatively into retrieval examples described in Part II.

Figures 6a–c, respectively, show sensitivities for an upper scattering layer at $\bar{p} = 0.35$ for optical depths $\tau_c = 0.1, 1.0, 10$, and for $a_{\text{sfc}} = 0.15, 0.6$. As a general rule, the radiance is sensitive to changes in surface albedo when the scattering layer is thin as indicated by the $\tau_c = 0.1$ and especially under weak absorption (i.e., small values of $\tau_{O_2}^*$). As absorption increases (e.g., $\tau_{O_2}^* > 1$), the effect of the surface albedo is diminished, leaving a response of the radiance largely determined by changes in the scattering layer properties itself. This is also the case for thick layers as surface effects become obscured by the scattering layer itself. Furthermore, the response of s_v to changes in these properties differs from that of I_v . Note that s_v is not as sensitive as I_v to surface albedo and, unlike the example discussed in relation to Figs. 5, the optical depth and phase function dependences begin to separate.

The sensitivities shown in Fig. 6a indicate that it is possible to distinguish optically thin layers above brighter lower reflecting surfaces (such as the ground or low cloud) which is a distinct advantage of a retrieval method that uses these measurements. We note, for example, how surface albedo effects on both observables separate spectrally from those effects introduced by changing layer scattering properties as the surface albedo is increased (from $a_{\text{sfc}} = 0.15$ to $a_{\text{sfc}} = 0.6$). The ability to distinguish high-level thin cloud over a bright-

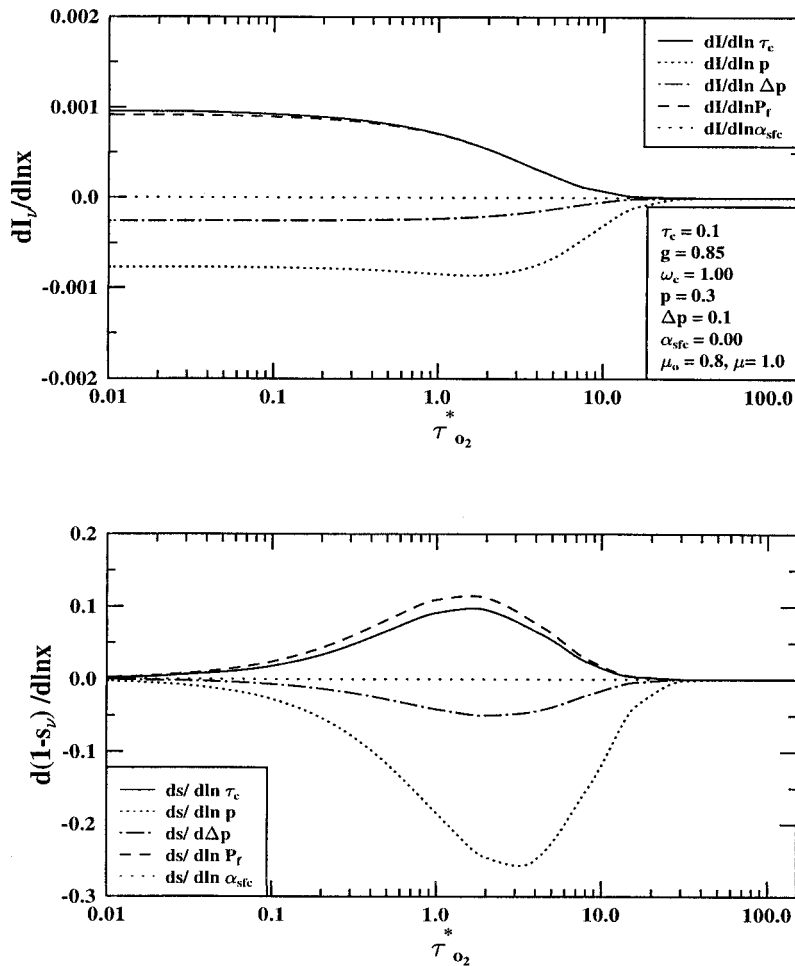


FIG. 5. Sensitivities of I_v and s_v to the optical layer and surface properties for high thin layer over a dark surface.

er lower-level cloud or reflecting surface is further demonstrated in Part II.

Corresponding sets of sensitivities for low-lying scattering layers located at $\bar{p} = 0.75$ are shown in Figs. 7a–c. On the whole, these are similar to those discussed for an upper layer except that both I_v and s_v show a greater sensitivity to changes in layer thickness owing to the relative increase in importance of absorption by O_2 in this lower layer. Furthermore, we might deduce from the results of both Figs. 6a–c and 7a–c is that any information about the vertical location of the scattering layer, such as information on the height and thickness, will greatly benefit any retrieval of the layer optical depth and optical properties. This issue is also explored further in Part II.

6. Effects of 3D geometry of the layer: The photon path lengths as a metric of horizontal homogeneity

The sensitivity results presented above and inferences drawn from them with regard to retrieval are ultimately

based on the assumption that the scattering layer is horizontally homogeneous with respect to the distribution of optical properties in that layer. Any proposed retrieval scheme that aims to derive cloud and aerosol properties from radiance measurements must address the extent to which this assumption affects the accuracy of the retrieval. This is a complex problem and we provide a preliminary assessment of the effects of 3D transport on the O_2 A-band reflection spectra. We now show how spectral radiances not only contain information about particle properties as described above but also provide some insight on 3D effects and the importance of these 3D effects on the retrievals.

a. Photon path statistics

We begin by couching the radiative transfer in terms of photon pathlength statistics. The path a photon travels in an absorbing medium is fundamental to the study of line absorption and the photon path length has proved to be a useful concept in past studies of absorbing lines

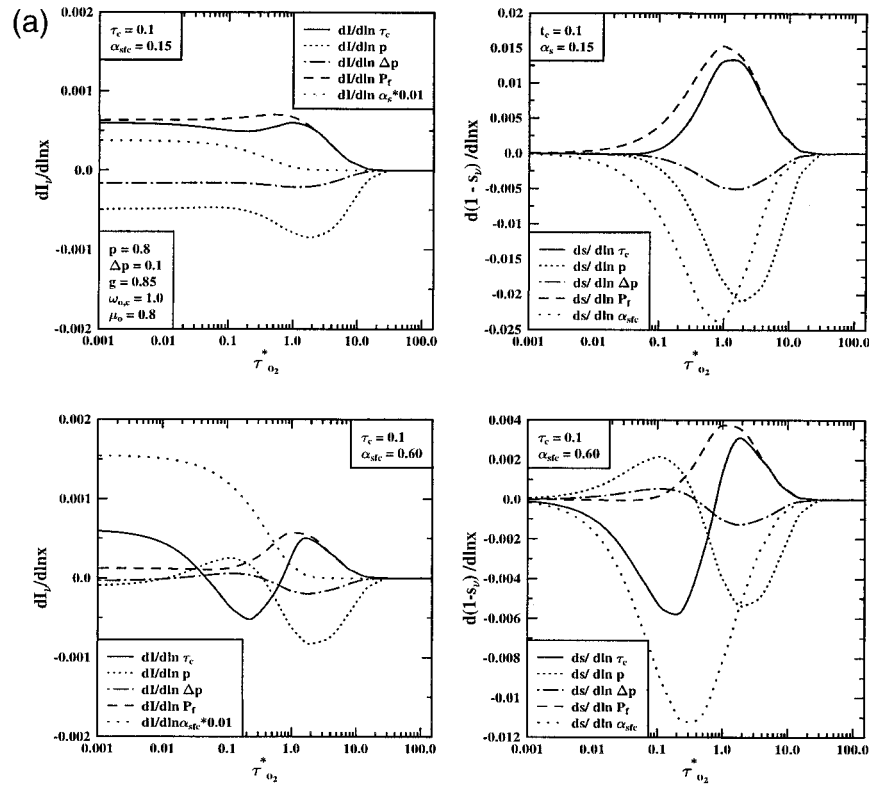


FIG. 6. (a) Sensitivities of I_ν and s_ν to the optical layer and surface properties for high thin layer ($\tau_c = 0.1$) over a land ($\alpha = 0.15$) and a bright ($\alpha = 0.60$) surface. (b) Sensitivities of I_ν and s_ν to the optical layer and surface properties for high moderately thick layer ($\tau_c = 1.0$) over

under the influence of multiple scattering (Irvine 1964, 1967; Fouquart and Lenoble 1973, among others).

The relevant path information is the function $p_\lambda(\lambda)d\lambda$ that represents the probability that a photon has traveled an optical path between λ and $\lambda + d\lambda$ and is defined such that

$$\int_0^\infty p_\lambda(\lambda) d\lambda = 1. \tag{23}$$

The mean photon (optical) pathlength then follows from this distribution as

$$\langle \lambda \rangle = \int_0^\infty \lambda p_\lambda(\lambda) d\lambda \tag{24}$$

and the ratio of $\langle \lambda \rangle$ to optical depth τ is a measure of the enhancement of the photon path by multiple scattering.

A comment on $p_\lambda(\lambda)$ is relevant here. The characteristics of this distribution not only depend on the properties of the scatterers including the 3D geometry under consideration but also on the radiometric quantity of interest. For example, photon path distributions for fluxes differ from those for radiances and differ according to the direction of the flow of radiation. The results

presented here apply to the radiances as observed by a nadir viewing instrument. Similar analysis for a ground-based instrument measuring zenith radiance is the topic of an ongoing study.

The properties of the path distributions relevant to plane-parallel geometry have been described in various papers and summarized by van de Hulst (1980). We present three examples of distributions derived for three optical depths, $\tau_c = 0.1, 1.0, 10$, in Fig. 8a. All other parameters used to produce the results of Fig. 5 were adopted and no particle absorption has been assumed. The distributions shown in Fig. 8a are derived using a backward Monte Carlo model (O'Brien 1992). The characteristics of these distributions for nadir reflectance have been described elsewhere (e.g., van de Hulst 1980). For $\tau_c = 0.1$, the distribution follows closely the single-scatter distribution (indicated by the dotted curve), which has a maximum value of $\lambda = m = 2.25\tau_c$ for the case shown. As τ_c increases, multiple scattering extends the tail of the distribution beyond the single-scatter limit (note that the single-scatter solution is not shown for the $\tau_c = 10$ case). Also shown in each panel for comparison is the distribution derived from isotropic scattering. Comparison between these distributions and those derived for an anisotropic phase function with g

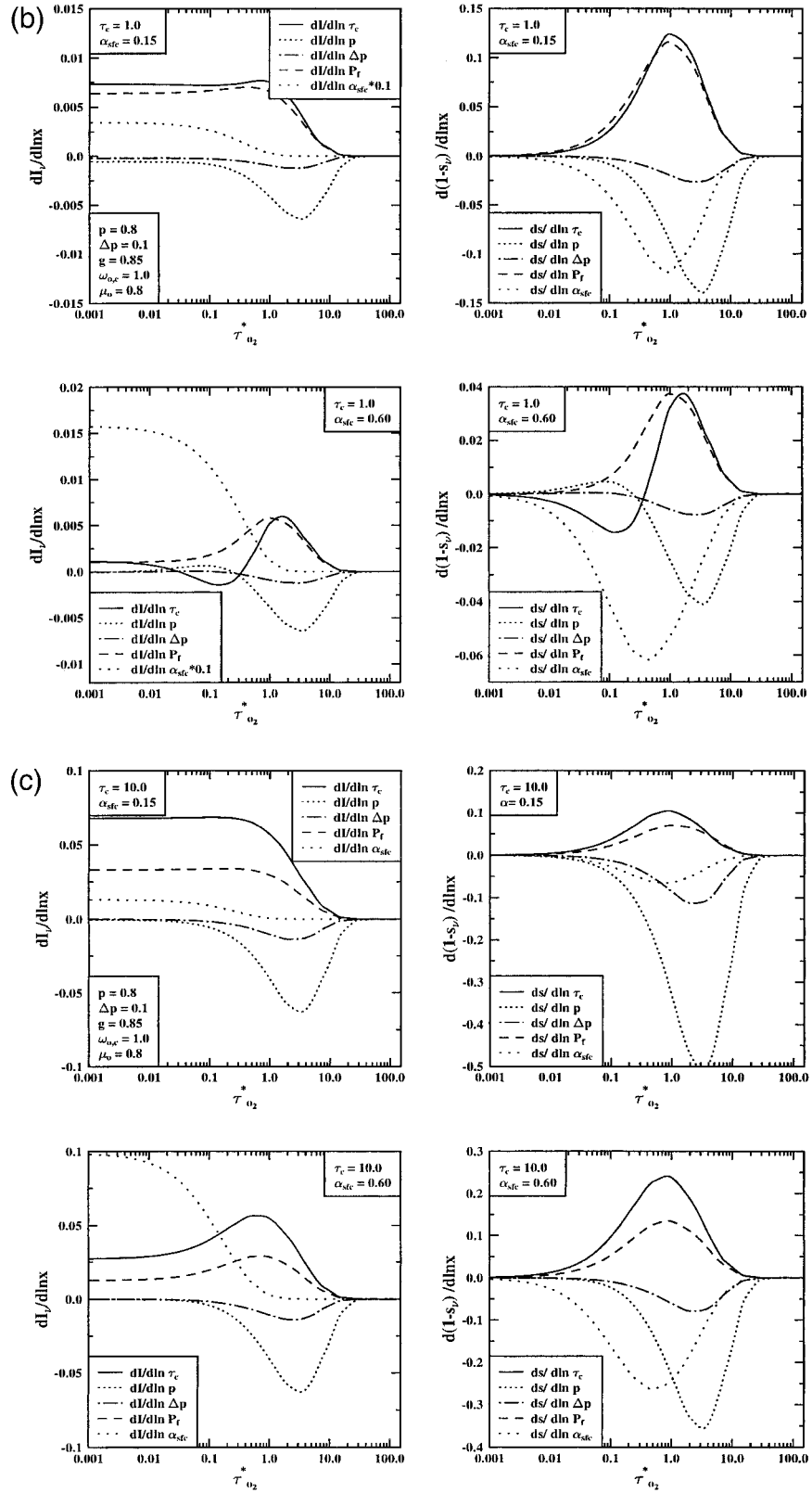


FIG. 6. (Continued) a land ($\alpha = 0.15$) and a bright ($\alpha = 0.60$) surface. (c) Sensitivities of I_v and s_v to the optical layer and surface properties for high thick layer ($\tau_c = 10.0$) over a land ($\alpha = 0.15$) and a bright ($\alpha = 0.60$) surface.

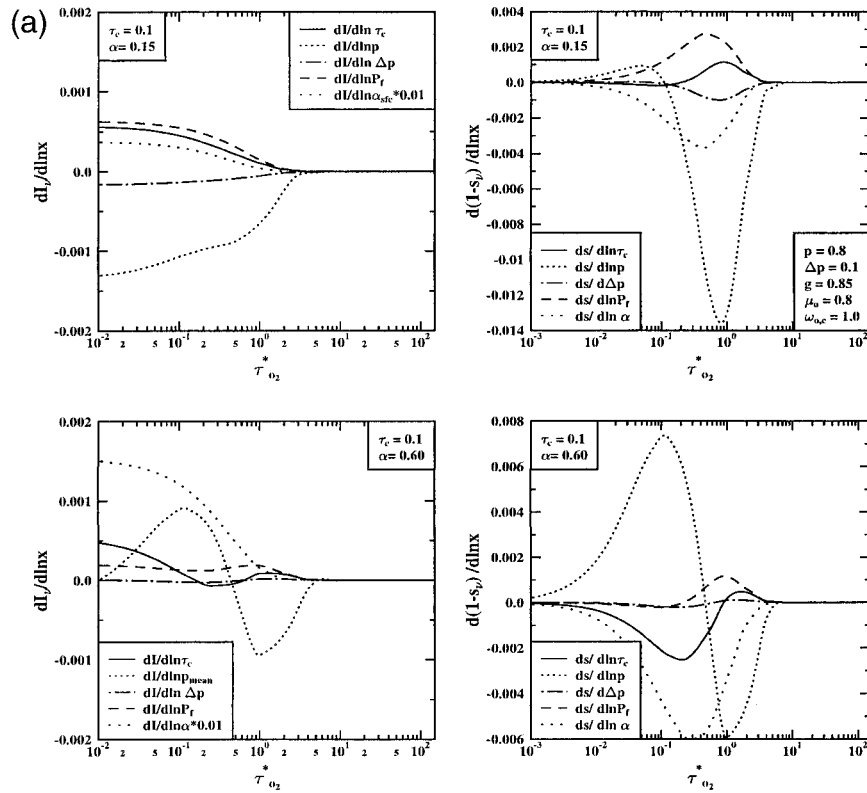


FIG. 7. (a) Sensitivities of I_v and s_v to the optical layer and surface properties for low thin layer ($\tau_c = 0.1$) over a land ($\alpha = 0.15$) and a bright ($\alpha = 0.60$) surface. (b) Sensitivities of I_v and s_v to the optical layer and surface properties for low moderately thick layer ($\tau_c = 1.0$) over a land

$= 0.85$ reveals how the distribution changes with the nature of the phase function.

An important aspect of the photon distributions is shown in Fig. 8b on which $\langle \lambda \rangle$ is plotted as a function of τ_c . The relation expressed by the solid line was derived from a series of doubling model calculations and is similar in nature to results presented by van de Hulst (1980). Under the assumption of plane-parallel geometry and for the specified solar geometry, there exists a distinct relation between the photon path and optical depth and that this relation is relatively insensitive to phase function as indicated by the closeness of the relationships derived for the two values of asymmetry parameter indicated.

b. The equivalence theorem

The equivalence theorem introduced by Irvine (1964) establishes a relation between radiances measured in a spectral region out of an absorption band (or between absorption lines) to a radiance measured within a line. This theorem is especially powerful when dealing with high spectral resolution simulations of 3D transport as considered below.

The dimensionless properties that enter this problem are the particle or continuum single-scatter albedo $\varpi_{o,c}$

$= \sigma_c / (\sigma_c + \kappa_c)$, the optical thickness outside the absorption band $\tau_c = \Delta z(\sigma_c + \kappa_c)$, the optical path outside the band, $\lambda = l(\sigma_c + \kappa_c)$ where l is the geometric path of the photon, and the optical path at a frequency ν inside the absorption band,

$$\lambda_\nu = l(\sigma_c + \kappa_c + \kappa_\nu) = \lambda(1 + \gamma_\nu),$$

where $\gamma_\nu = \kappa_\nu / \sigma_c + \kappa_c$ is the ratio of the line absorption to particle extinction.

The equivalence theorem states that with introduction of absorption without changing either the geometry of the medium or scattering properties of the medium, the radiance along a given direction ξ is

$$I(\varpi_o \neq 1, \xi) = I(\varpi_o = 1, \xi) \int_0^\infty p(\lambda) \mathcal{T}(\lambda) d\lambda, \quad (25)$$

where we introduce a transmission function

$$\mathcal{T}(\lambda) = \exp(-\gamma\lambda)$$

that depends only on optical path length λ and is the transmission function representing the effects of gas (true) absorption. Thus the radiance in an absorbing line follows directly from knowledge of the photon path distributions and the radiance associated with the transfer derived outside absorption lines. The theorem embodied

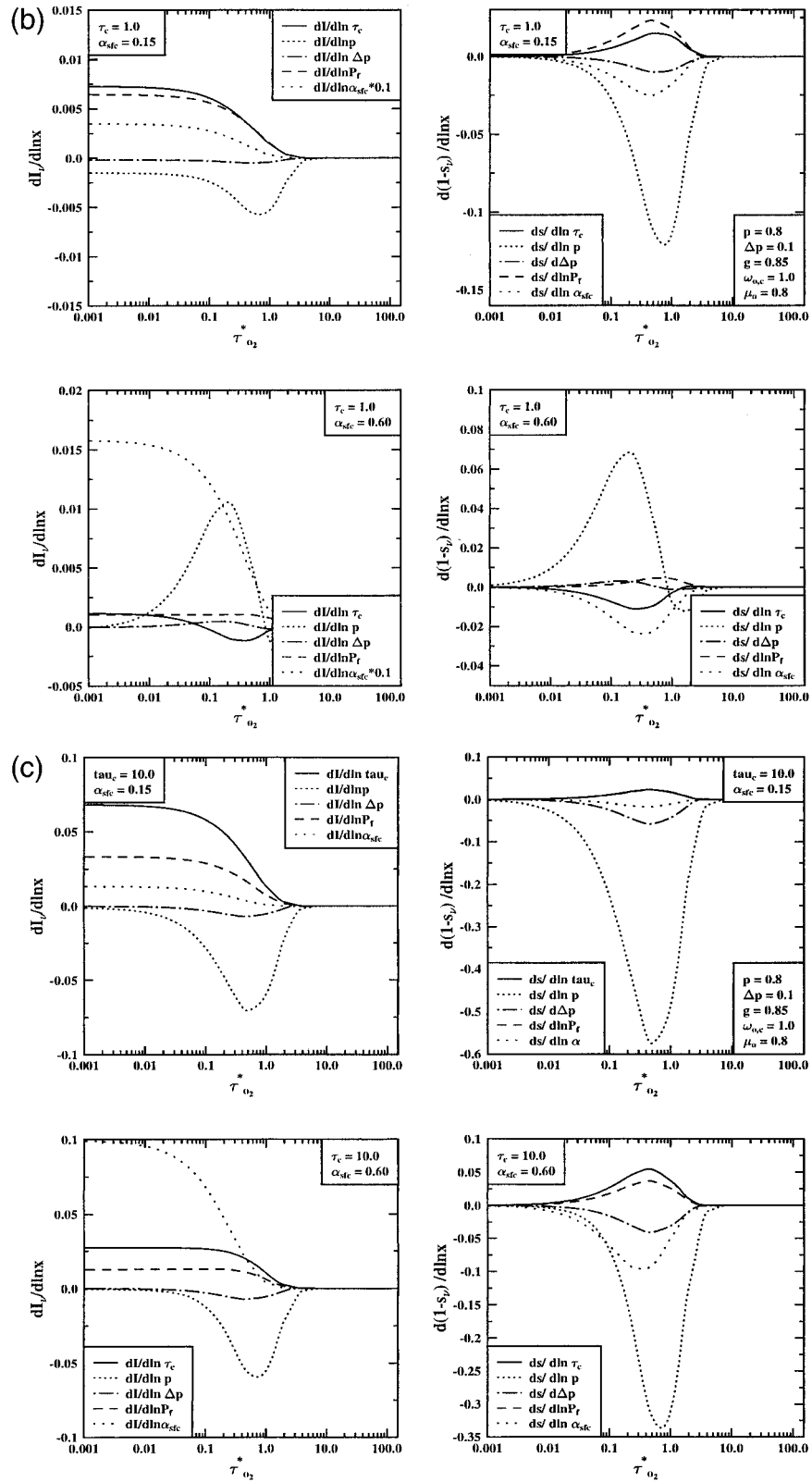


FIG. 7. (Continued) ($\alpha = 0.15$) and a bright ($\alpha = 0.60$) surface. (c) Sensitivities of I_v and s_p to the optical layer and surface properties for low thick layer ($\tau_c = 10.0$) over a land ($\alpha = 0.15$) and a bright ($\alpha = 0.60$) surface.

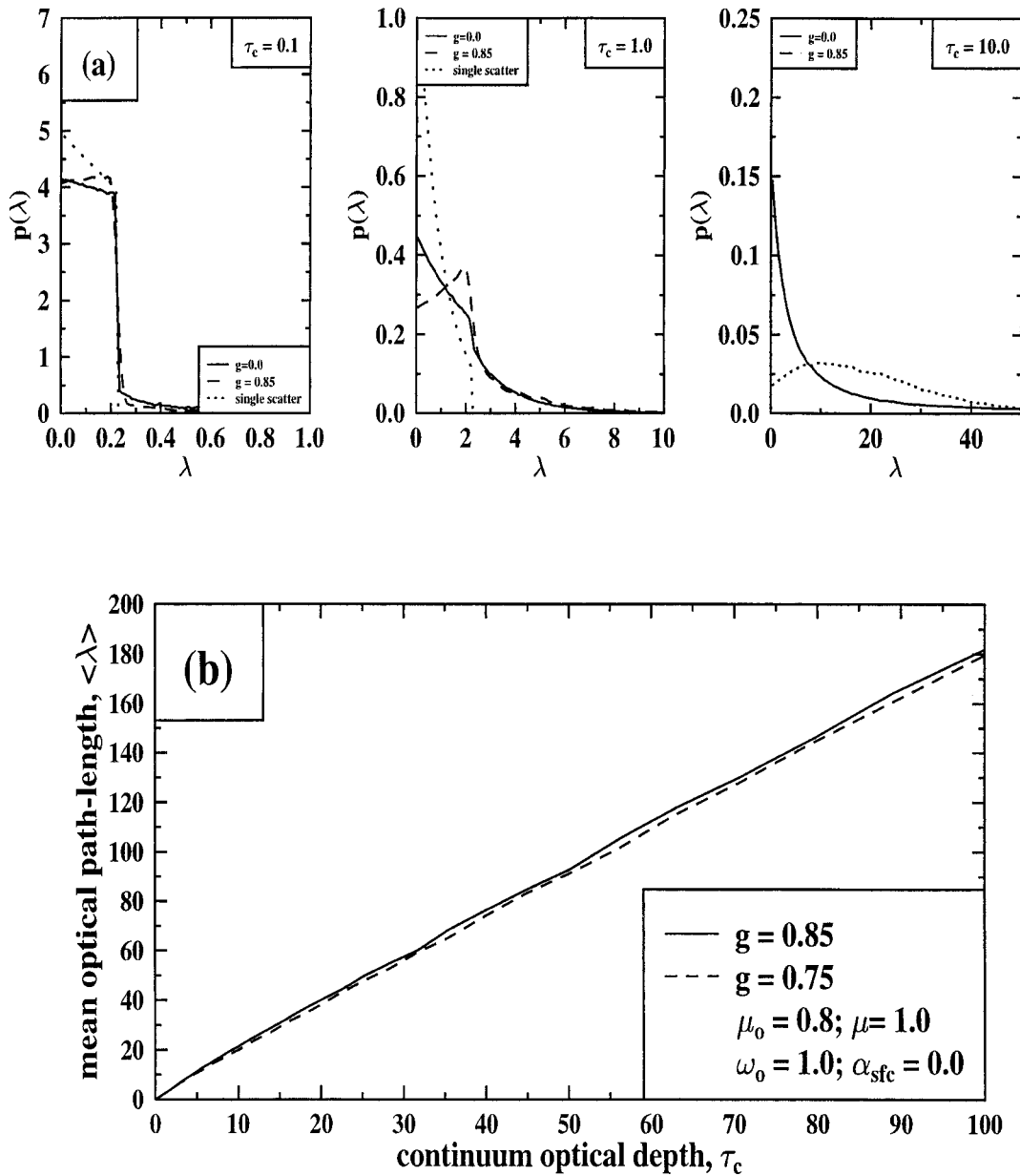


FIG. 8. Variation of pathlength distributions and optical depth and asymmetry parameter (a). Variation of mean pathlength, $\langle \lambda \rangle$ as a function of continuum optical depth, τ_c (b).

in (25) is formally rigorous and independent of any assumption about the geometry of the medium. In principle only one scattering transfer problem is required to simulate a spectrum (assuming particle properties are constant across the spectral region of interest).

An illustration of the utility of the equivalence theorem is provided in Fig. 9. The upper panel of that diagram presents simulated reflection spectra as a function of wavenumber and the lower panel presents the same spectra reorganized as a function of O_2 optical depth, providing a clearer presentation of the results.

Two simulations are presented in each panel and the quantities plotted are $1 - s_p$. The solid continuous line corresponds to the reflection spectra produced from the doubling-adding model for a single cloud layer of optical depth $\tau_c = 4.0$ and for other parameters as stated on the diagram. The individual points represent the evaluation of (25) using the photon path distribution as given in Fig. 8. In this case only one scattering calculation is required to derive $p(\lambda)d\lambda$ and the entire reflection spectrum is produced from this single distribution. The agreement is essentially exact with numerical differ-

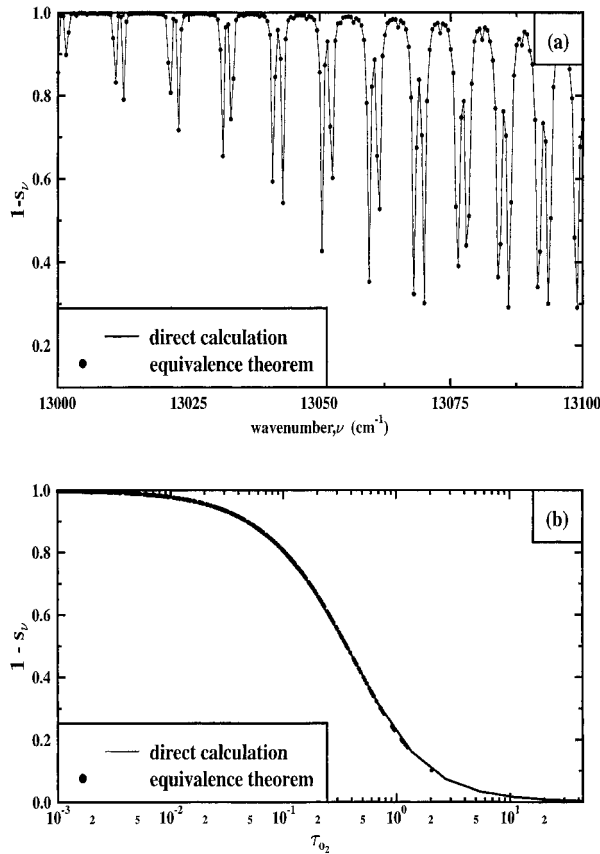


FIG. 9. Comparison of absorption spectra computed directly and from the equivalence theorem Eq. (25) (a). Same as (a) except reordered with respect to absorption optical thickness, τ_{o_2} .

ences between the two spectra too small to be meaningful.

c. Results for 3D geometry and spectral metrics of homogeneity

The effects of horizontal variability of the scattering layer on the radiative transfer, expressed here in terms of $p(\lambda)d\lambda$ are highlighted in Fig. 10. The path distributions presented correspond to the three hypothetical cloud distributions shown in the form of images of the horizontal distribution of optical depth. The cloud occupied a single layer and was located between 900 and 800 hPa in a model atmosphere. The horizontal distributions were created using a simple mass-conserving fractal scheme (Cahalan 1989). The simulated cloud fields generated represent a reasonable range of heterogeneity typical of boundary layer clouds and were constructed on a 250×250 grid. The mean optical depth in each case is 4 and cyclic boundary conditions were assumed in the radiative transfer computations that were performed using the backward Monte Carlo model to arrive at the pathlength distributions at each grid point for a nonabsorbing wavelength. Line-by-line spectra

were derived for each grid point from the grid point path distributions via the equivalence theorem. Vertical variations in extinction were ignored in these simulations.

It follows from (25) that the photon path distribution may be obtained from measurements of s_ν , or more precisely $1 - s_\nu$, via the inverse Laplace transform of (25) (e.g., van de Hulst 1980; Bakan and Quenzel 1976, among others). According to van de Hulst (1980), the mean optical path may be obtained as

$$\langle \lambda \rangle = -\tau_c (1 + \gamma) \frac{\partial \ln s_\nu}{\partial \tau_\nu(0, 1)} \quad (26)$$

for $\gamma \rightarrow 0$ and assuming that the product $\omega_{o,\nu} \tau_\nu^*$ remains constant as is the case for an absorption feature in a uniform continuum. Since τ_c is a constant, γ is directly proportional to O_2 optical depth. Figure 11 illustrates (26) showing $\langle \lambda \rangle$ as a function of the O_2 optical depth for a single layer of atmosphere containing a cloud. The solid points are the pathlengths derived for a plane-parallel cloud and the cross symbols correspond to the 3D cloud field 2 of Fig. 10. The quantities were derived using a Monte Carlo model and the equivalence theorem to determine the spectrum of s_ν . The photon pathlength was obtained from a numerical evaluation of (26) applied to this spectrum. As expected, $\langle \lambda \rangle$ decreases as the absorption is increased. In the absence of absorption (i.e., $\tau_\nu \rightarrow 0$), the effect of 3D structure on reflection is to enhance the photon path. This enhancement decreases as the absorption is increased. When the absorption is strong enough, the effects of horizontal variability are minimized. At these wavelengths, the radiative transfer is well approximated by plane-parallel radiative transfer.

We now describe how pathlength information, together with optical depth information retrieved from radiance data, might be used as a way of identifying potential adverse effects of horizontal inhomogeneity on retrievals. The analysis is based on the observation that effects of horizontal geometry lead to (i) reduced reflected radiances with a subsequent *negative bias* in inferred optical depth (e.g. Cahalan et al. 1994). This is shown in Fig. 12a for the clouds presented in Fig. 10. The optical depth is retrieved via the method described in Part II and is lower than the actual mean optical depth corresponding to that retrieved for perfect plane-parallel conditions. The magnitude of the bias increases as the horizontal heterogeneity increases. (ii) The second piece of information of relevance is the relationship between mean photon path and optical depth as shown previously in Fig. 8b. It is possible to use this relationship to estimate optical depth given $\langle \lambda \rangle$. Effects of horizontal geometry leads to enhanced values of $\langle \lambda \rangle$ compared to the plane-parallel counterpart and this leads to a *positive bias* in optical depth as shown in Fig. 12b. Thus the sense of the nonplane-parallel bias is opposite in reflection and pathlength and the differ-

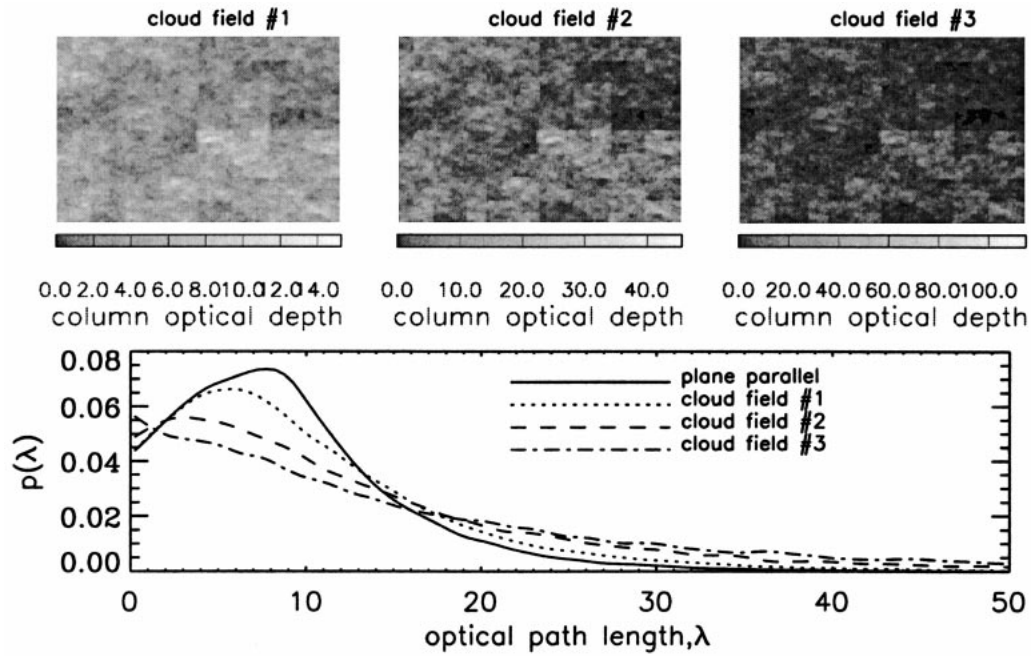


FIG. 10. Horizontal distribution of column optical depth for three inhomogeneous cloud fields with the same mean optical depth ($\langle \lambda_c \rangle = 4$) (a). Variation of domain-averaged photon pathlength distribution for each cloud field (b).

ence in the estimated optical depths $\Delta_\tau = \tau_{\text{refl}} - \tau_{\langle \lambda \rangle}$ might be considered to be a simple measure of horizontal heterogeneity. In this definition, τ_{refl} refers to the optical depth estimate based on reflected radiances and $\tau_{\langle \lambda \rangle}$ refers to estimates of optical depth based on mean

pathlengths. Under perfect plane-parallel conditions $\Delta_\tau = \varepsilon$ where ε is the intrinsic error of the retrievals. In principle, $\varepsilon = 0$; however, in practice, errors arise for reasons discussed in Part II.

7. Summary and conclusions

This paper analyzes the reflection spectrum associated with sunlight reflected from the atmosphere in the O₂ A band. The intent of the study reported in this paper is to revisit the classical problem of particle scattering–gaseous absorption and consider the extent to which line absorption properties can be used to obtain information about particle scatterers. This is a different slant to the problem most typically considered in relation to A-band spectroscopy. The work is based on the earlier conclusions of O’Brien and Mitchell (1992), who showed how the O₂ reflection spectrum itself, if observed with sufficient spectral resolution, contains information sufficient to deconvolve the effects of particles for the absorption by O₂. The spectral resolution needed is beyond that of current A-band spectrometers.

The results presented in this paper provide the theoretical foundation for the retrieval of particle information from spectral measurements of line absorption pursued in a related paper (Heidinger and Stephens 2000). The paper provides a limited background discussion on the O₂ absorption spectrum and presents a simple atmospheric model of this absorption and discusses this absorption in terms of two related observables: the spectral radiance and the line profile, which is a ratio of spectral radiances obtained in and outside

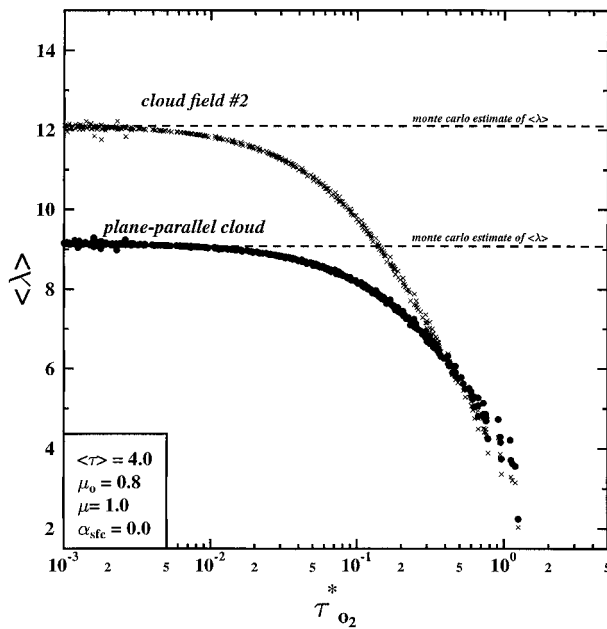


FIG. 11. Spectral variation of mean pathlength with absorption optical depth for cloud field 2 in Fig. 10 and a plane-parallel cloud with identical optical properties. Dashed lines show Monte Carlo estimates of $\langle \lambda \rangle$ in the continuum.

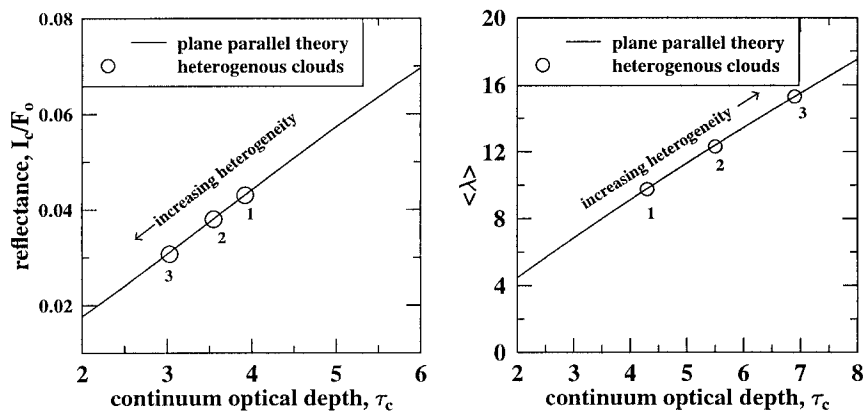


FIG. 12. The effect of cloud heterogeneity on the reflectances and mean photon pathlengths for the cloud fields shown in Fig. 10 compared to plane-parallel theory.

absorbing lines. The absorption model is incorporated into two simple scattering models; namely, the single-scatter model approximating optically thin cloud and aerosol layers and the semi-infinite isotropic model of Chandrasekhar to represent an optically thick cloud. Both serve to identify the following key properties that define the spectra: (i) the optical depth of the cloud or aerosol, (ii) the pressure level of the top of the cloud or aerosol which defines the O_2 optical depth above the scattering layer, (iii) the surface albedo, (iv) the scattering phase function, and (v) the pressure thickness of the scattering layer or, more precisely, the optical depth of oxygen in this layer.

The relevant conclusions that can be drawn from this study are the following.

- 1) Crucial to any retrieval scheme that uses input measurables in the form of either I_v and s_v , is the sensitivity of these measurables to changes in these five parameters. We show how the sensitivities of both the spectral radiance and the radiance ratio line parameter to changes in the above-mentioned parameters vary according to the O_2 optical depth and it is the variation of these sensitivities across the spectrum that is a key developing a method to retrieve these parameters. Thus spectral measurements that resolve the range in absorption therefore offer potential for separating the dependence of the measurements on these parameters, thereby providing some basis for their retrieval.
- 2) The radiance reflected from thin layers is sensitive to optical depth and phase function whereas the ratio is sensitive to layer height. For thick layers, the sensitivity to optical depth diminishes, leaving primarily a sensitivity to bulk information about the scattering phase function. Both quantities are sensitive to surface albedo but this sensitivity diminishes as O_2 absorption increases. In this case, the response of the radiance is largely determined by changes in the scattering layer properties itself. This is also the case for

thick layers as surface effects become obscured by the scattering layer itself.

- 3) A consequence of 2) above is that by measuring radiances as a function of changing O_2 absorption, it is possible to distinguish optically thin layers above brighter lower reflecting surfaces. The ability to distinguish high-level thin cloud over a brighter lower-level cloud or reflecting surface is further demonstrated in Part II.
- 4) In general any information on the height and thickness of the scattering layer, such as might be available from concurrent measurements from a lidar or cloud radar, is likely to benefit the retrieval of the layer optical depth and optical properties.
- 5) The effects of 3D geometry on the spectral radiances is considered in the context of photon path. It is shown how the spectral radiances provide some insight on 3D effects and the importance of these 3D effects on the retrievals. The equivalence theorem is illustrated and is used to provide line-by-line simulations of the reflection spectrum from hypothetical 3D clouds. When the O_2 optical depth exceeds a value of about 4, 3D effects are negligible (relative to plane-parallel clouds).
- 6) The effects of 3D geometry introduce biases in the optical depth estimated using reflected radiances and alternatively estimated using photon path information. These biases are in the opposite sense (a negative albedo optical depth bias and positive photon path optical depth bias). It is suggested that the difference between the two values of optical depth derived by these alternate methods is a metric of 3D effects on the radiative transport.

Acknowledgments. Early portions of this research were supported under NASA Grant NAG1-1702. The bulk of this research has been supported under NASA Grant NAG1-1849 under Contract PNO 34402.

REFERENCES

- Bakan, S., and H. Quenzel, 1976: Path length distributions of photons scattered in turbid atmospheres. *Contrib. Atmos. Phys.*, **49**, 272–284.
- Cahalan, R. F., 1989: Overview of fractal clouds. *Remote Sensing Retrieval Methods*, A. Deepak, Ed., A. Deepak Publishing, 371–389.
- , W. Ridgway, W. Wiscombe, T. L. Bell, and J. B. Snider, 1994: The albedo of fractal stratocumulus clouds. *J. Atmos. Sci.*, **51**, 2434–2455.
- Chamberlain, J. W., and D. M. Hunten, 1987: *Theory of Planetary Atmospheres*. 2d ed. Academic Press, 481 pp.
- Chance, K., J. P. Burrows, D. Perner, and W. Schneider, 1997: Satellite measurements of atmospheric ozone profiles, including tropospheric ozone, from ultraviolet/visible measurements in the nadir geometry: A potential method to retrieve tropospheric ozone. *J. Quant. Spectrosc. Radiat. Transfer*, **57**, 467–476.
- Chandrasekhar, S., 1960: *Radiative Transfer*. Dover, 393 pp.
- Fischer, J., and H. Grassl, 1991: Detection of cloud-top height from backscattered radiances within the oxygen-A band. Part I: Theoretical study. *J. Appl. Meteor.*, **30**, 1245–1259.
- Fouquart, Y., and J. Lenoble, 1973: Formation des raies spectrales et étude des courbes de croissance dans une atmosphère diffusante semi-infinie. *J. Quant. Spectrosc. Radiat. Transfer*, **13**, 447–459.
- Goody, R. M., and Y. L. Yung, 1989: *Atmospheric Radiation: Theoretical Basis*. Oxford University Press, 519 pp.
- Heidinger, A. K., and G. L. Stephens, 2000: Molecular line absorption in a scattering atmosphere. Part II: Application to remote sensing in the O₂ A band. *J. Atmos. Sci.*, **57**, 1615–1634.
- Irvine, W. M., 1964: The formation of absorption bands and the distribution of photon optical paths in a scattering atmosphere. *Bull. Astron. Inst. Neth.*, **17**, 266–279.
- , 1967: Absorption bands and photon optical paths in a non-conservative scattering atmosphere. *Astrophys. J.*, **147**, 1193–1197.
- Lacis, A. A., and V. Oinas, 1991: A description of the correlated k distribution method for modeling nongray gaseous absorption, thermal emission, and multiple scattering in vertically inhomogeneous atmosphere. *J. Geophys. Res.*, **96** (D5), 9027–9063.
- Liou, K. N., Y. Takano, W. Gellerman, R. M. Goody, G. L. Stephens, and R. West, 1997: On the information content of thin cirrus reflectance in the 1.4 μm water vapor band. Preprints, *Ninth Conf. on Atmospheric Radiation*, Long Beach, CA, Amer. Meteor. Soc., 267–269.
- McClatchey, R., and Coauthors, 1972: Optical properties of the atmosphere. 3d ed. AFCRL-72-0497, Air Force Cambridge Research Labs., 107 pp.
- Mitchell, R. M., and D. M. O'Brien, 1987: Error estimate for passive satellite measurements of surface pressure using absorption in the A band of oxygen. *J. Atmos. Sci.*, **44**, 1981–1991.
- O'Brien, D. M., 1992: Accelerated quasi Monte Carlo integration of the radiative transfer equation. *J. Quant. Spectrosc. Radiat. Transfer*, **48**, 41–59.
- , and R. M. Mitchell, 1992: Error estimates for retrieval of cloud-top pressure using absorption in the A-band of oxygen. *J. Appl. Meteor.*, **31**, 1179–1192.
- Ramaswamy, V., and S. M. Freidenreich, 1991: Solar radiative line-by-line determination of water vapor absorption and water cloud extinction in inhomogeneous atmospheres. *J. Geophys. Res.*, **96**, 9133–9157.
- Rothman, L. S., and Coauthors, 1987: The HITRAN molecular database: Editions of 1991 and 1992. *J. Quant. Spectrosc. Radiat. Transfer*, **48**, 469–507.
- Stephens, G. L., 1994: *Remote Sensing of the Lower Atmosphere: An Introduction*. Oxford University Press, 523 pp.
- van de Hulst, H. C., 1980: *Multiple Light Scattering: Tables, Formulas, and Applications*. Vol. II. Academic Press, 436 pp.
- Wu, M.-L. C., 1985: Remote sensing of cloud-top pressure using reflected solar radiation in the oxygen A-band. *J. Climate Appl. Meteor.*, **24**, 539–546.
- Yamamoto, G. A., and D. Q. Wark, 1961: Discussion of the letter by R. A. Hanel, "Determination of cloud altitude from a satellite." *J. Geophys. Res.*, **66**, 3596.